Interactions of Dimethylsulfoxide with a Dipalmitoylphosphatidylcholine Monolayer Studied by Vibrational Sum Frequency Generation†

Xiangke Chen and Heather C. Allen*

The Ohio State University, Department of Chemistry, 100 West 18th Avenue, Columbus, Ohio 43210

Received: May 29, 2009; Revised Manuscript Received: August 19, 2009

The interactions between phospholipid monolayers and dimethylsulfoxide (DMSO) molecules were investigated by vibrational sum frequency generation (VSFG) spectroscopy in a Langmuir trough system. Both the head and the tail groups of dipalmitoylphosphatidylcholine (DPPC) as well as DMSO were probed to provide a comprehensive understanding of the interactions between DPPC and DMSO molecules. A condensing effect is observed for the DPPC monolayer on a concentrated DMSO subphase (>20 mol %). This effect results in a well-ordered conformation for the DPPC alkyl chains at very large mean molecular areas. Interactions between DMSO and DPPC headgroups were also studied. DMSO-induced dehydration of the DPPC phosphate group is revealed at DMSO concentration above 10 mol %. The average orientation of DMSO with DPPC versus dipalmitoylphosphate sodium salt (DPPA) monolayers was compared. The comparison revealed that DMSO molecules are perturbed and reorient because of the interfacial electric field created by the charged lipid headgroups. The orientation of the DPPC alkyl chains remains nearly unchanged in the liquid condensed phase with the addition of DMSO. This suggests that DMSO molecules are expelled from the condensed monolayer. In addition, implications for the DMSO-induced permeability enhancement of biological membranes from this work are discussed.

Introduction

Dimethylsulfoxide (DMSO) is considered to be a universal solvent and has found wide applications in pharmaceutical and biological sciences. The DMSO molecule consists of a polar S═O moiety and two nonpolar CH_3 groups. Such small amphiphilic structure makes it feasible for DMSO molecules to incorporate into the lipid−water interface and therefore to penetrate into the cell membrane. As the most common cryoprotectant, DMSO is used for preservation of biological tissues at low temperature.[1–4] DMSO can penetrate into the cell interior and is therefore perceived to protect the cell by preventing ice formation in extracellular and intracellular spaces.[5] DMSO has been used to improve drug delivery in diverse types of membranes[6–9] and has been shown to be effective in promoting the penetration of both hydrophilic and lipophilic substances.[10] Moreover, DMSO is known as an agent that induces cell fusion[11] and promotes cell differentiation.[12] Given the importance of DMSO in various practical applications, the molecular level mechanisms responsible for these effects have been of great interest.[13]

It is generally thought that DMSO influences the structure and properties of membranes. The interaction of DMSO with model membranes has been previously studied by various experimental and theoretical approaches, that is, differential scanning calorimetry (DSC),[14–16] X-ray diffraction (XRD),[14,15,17,18] small-angle neutron diffraction,[19,20] nuclear magnetic resonance (NMR),[21] infrared (IR) spectroscopy,[16] and molecular dynamics (MD) simulations.[22–27] As one of the most common phospholipids, dipalmitoylphosphatidylcholine (DPPC) is often used in model biological membrane systems in research. The influence of DMSO on DPPC model membranes was shown to be concentration-dependent, and significant structural changes to the membranes were observed in aqueous solutions of DMSO <30 mol %.[17,28] The temperature of the main phase transition of DPPC vesicles in water/DMSO mixed solvent increases with DMSO concentration, revealing a stabilization effect by DMSO on the vesicle gel phase.[7,14] X-ray and neutron diffraction studies revealed that the repeat distance between the bilayers in multilamellar DPPC vesicles decreased with DMSO concentration. This decrease in intermembrane distance inside the vesicles was mainly attributed to the decrease in the intermembrane solvent layer thickness, namely, the removal of free water molecules in the intermembrane spaces.[17,20]

In addition to experimental efforts, MD simulations provide more insight. Sum et al. showed that DMSO penetrates readily into the polar headgroup region of a DPPC bilayer, but only a few DMSO molecules actually cross the bilayer.[25] Most recently, Anwar and coworkers reported water pore formation within a DPPC bilayer induced by DMSO using MD simulation.[26,27] This finding presented an interesting explanation of the enhanced transdermal permeability by DMSO, which casts light on the molecular interaction between DPPC and DMSO molecules.

Although many efforts have been made, probing the intermolecular interactions between DMSO and lipid model membranes directly in the interfacial region has not been reported; a molecular-specific technique is required to meet this need. Vibrational sum frequency generation (VSFG) is a powerful surface-selective and molecular-specific technique that has been successfully applied in many phospholipid studies.[29–32] As a second-order optical spectroscopy, VSFG intensity arises from the lack of inversion symmetry. Unlike in bulk solution, inversion symmetry is broken at a surface. This gives rise to the surface selectivity of VSFG. A perfect lipid bilayer is centrosymmetric and thus VSFG inactive;[33–35] therefore, lipid monolayers instead of bilayers are often used as model systems in VSFG studies.

† Part of the "Russell M. Pitzer Festschrift".

* Corresponding author. E-mail: allen@chemistry.ohio-state.edu.

10.1021/jp905066w CCC: $40.75
Published on Web 09/14/2009

SCHEME 1: Molecular Structures of DPPC and DPPA[a]

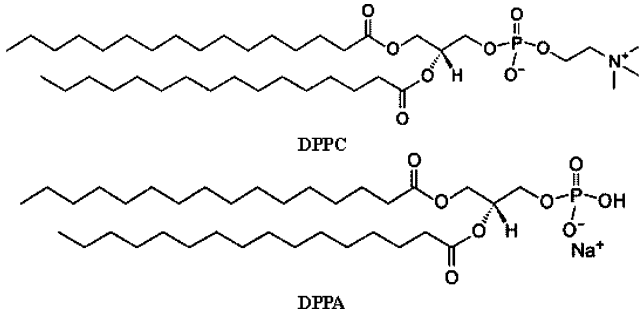

[a] DPPC-d_{62} and DPPA-d_{62} refer to the 62 hydrogens on the chains being replaced by 62 deuteriums.

Previous studies of DMSO−membrane interactions mainly focused on the gel phase of bilayers. The gel phase and fluid phase of a bilayer are analogous to the liquid condensed phase and liquid expanded phase of a monolayer, respectively. The use of the Langmuir trough allows us to investigate the monolayer in the liquid condensed phase and in the liquid expanded phase. In this article, we study the interaction between DMSO and DPPC molecules in monolayers by VSFG spectroscopy coupled to a Langmuir trough. A series of water/DMSO subphases was used to examine the concentration-dependent effect of DMSO on phospholipid monolayer structure. Both the head and tail groups of the DPPC molecules as well as DMSO molecules were probed to elucidate the interactions between the DMSO and the DPPC molecules.

Experimental Section

Materials. DMSO (>99% purity) was purchased from Fisher. 1,2-Dipalmitoyl-*sn*-glycero-3-phosphocholine (DPPC) was obtained from Avanti Polar Lipids (Alabaster, AL). Chain fully deuterated 1,2-dipalmitoyl-*sn*-glycero-3-phosphocholine (DPPC-d_{62}) and 1,2-dipalmitoyl-*sn*-glycero-3-phosphate sodium salt (DPPA-d_{62}) were also purchased from Avanti Polar Lipids. Molecular structures of DPPC and DPPA are shown in Scheme 1. Spectrophotometric grade chloroform was purchased from Sigma-Aldrich. Deionized water (not purged of CO_2) with a resistivity of 18.2 MΩ·cm and a measured pH of 5.5 was from a Barnstead Nanopure system.

Method. The surface pressure−area isotherm was obtained with a KSV minitrough (KSV, Finland). The rectangular trough (176.5 × 85 mm^2) is made of Teflon, and two barriers are employed to provide symmetric film compression. The barriers, which are made of Delrin, prevent leakage of the monolayer. The surface pressure and mean molecular area (MMA) were continuously monitored during film compression by the Wilhelmy plate method. The trough was filled with Nanopure water as the subphase. The surface pressure−area isotherm was always measured on a fresh subphase. Before lipids were spread on the surface, the fresh subphase surface was swept by the barriers to make sure that there was no significant surface pressure increase observed upon compression. The compression rate of the barrier to obtain the isotherms was 5 mm/min. Compression rates as low as 1 mm/min were used to check (data not shown) the reproducibility of the isotherm including the collapse pressure. Before recording an isotherm, we zeroed the surface pressure for each subphase. The sample temperature was maintained at 22 ± 1 °C for isotherm and VSFG measurements.

The broad bandwidth VSFG system[36–38] consists of two 1 kHz repetition rate regenerative amplifiers (Spectra-Physics Spitfire, femtosecond and picosecond versions), both of which are seeded by sub-50 fs 792 nm pulses (wavelength is tuned for system optimization) from a Ti/sapphire oscillator (Spectra-Physics, Tsunami) and pumped by a 527 nm beam from an all solid-state Nd/YLF laser (Spectra-Physics, Evolution 30). The two regenerative amplifiers provide 85 fs pulses and 2 ps pulses at 792 nm. The spectrally broad femtosecond pulses are used to drive the IR generation in an OPA (optical parametric amplifier; TOPAS, Quantronix) and then produce broad bandwidth IR pulses (~200 cm^{-1} fwhm). Stable IR pulses are tunable in various wavelength regions ranging from 1000 to 3800 cm^{-1}. The output energy of each 792 nm picosecond pulse was set to 300 μJ, and the IR energies were ~9 μJ in the C−H stretching region and ~3 μJ in the PO_2^- symmetric stretching region at the sample stage.

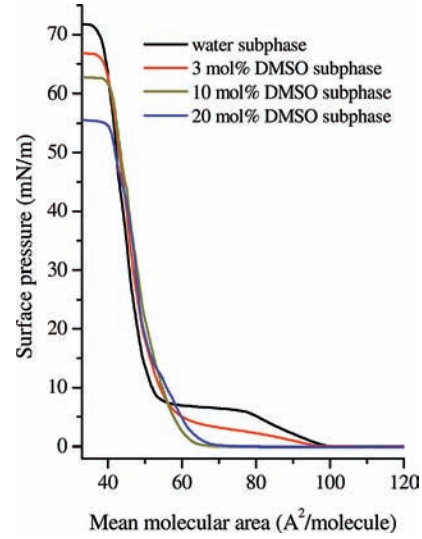

Figure 1. Isotherms of DPPC monolayers on different DMSO/water subphases.

The VSFG spectrum is polarization-dependent. In this study, spectra with the polarization combination of *ssp* (*s*-SFG; *s*-visible; *p*-infrared) are shown. The *ppp* polarization combination (data not shown) was used to verify assignments and orientation. Spectral resolution was 8 cm^{-1}.[39] The VSFG spectra were normalized against a nonresonant VSFG spectrum from a GaAs crystal (Lambda Precision Optics) to remove the spectral distortion caused by the energy profile of the IR pulse. To calibrate the VSFG peak positions, a nonresonant VSFG spectrum from the GaAs crystal surface was obtained with a polystyrene film covering the OPA IR output port. The resulting VSFG spectrum containing polystyrene IR absorption bands was used for the calibration. When performing a VSFG study on the monolayer in dynamic compression mode, the spectra were taken under either the pause working mode of the film balance or the hold working mode of the film balance. Each VSFG spectrum is obtained in a 1 min acquisition time, and all spectra reported are the average of five consecutive runs.

Results and Discussion

Compression Isotherms. The interactions between DMSO and DPPC molecules influence the phase behavior of DPPC Langmuir monolayers. The phase behavior can be characterized by surface pressure−area isotherm measurements. The surface pressure−area isotherms of DPPC monolayers on subphases containing different DMSO concentrations are shown in Figure 1. The isotherm of a DPPC monolayer on a pure water subphase (black trace) shows several distinct phases, which are generally

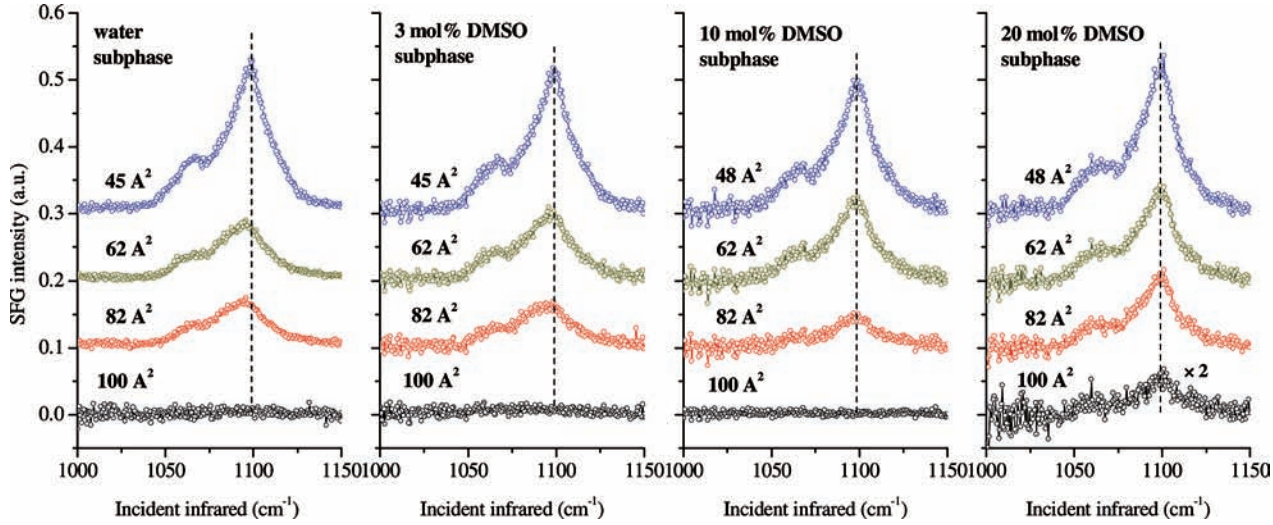

Figure 2. P═O region VSFG spectra of DPPC monolayers on different DMSO/water subphases at different surface coverages. From left to right, the subphases are water and 3, 10, and 20 mol % DMSO, respectively. The dashed line shows the $-PO_2^-$ SS peak position in the liquid condensed phase. (DPPC is in the LC phase at 45 and 48 Å^2/molecule.)

assigned to the gas (G, > 120 Å^2/molecule, not shown in Figure 1) phase, the gas−liquid expanded coexistence (G−LE) region, the liquid expanded (LE) phase, the liquid expanded−liquid condensed coexistence (LE−LC) region, the liquid condensed (LC) phase, and the collapse phase. As the DPPC monolayer is compressed, the surface pressure (difference between the surface tension of the subphase and the monolayer covered surface) rises when entering the LE phase. The first-order LE−LC phase transition occurs at ~6 mN/m at the experiment temperature of 22 °C, and collapse occurs at ~72 mN/m.

Isotherms of DPPC monolayers on 3, 10, and 20 mol % DMSO/water mixed subphases are shown in red, green, and blue in Figure 1, respectively. With the addition of 3 mol % DMSO in the subphase, the surface pressure of the LE to LC phase transition plateau (LE−LC region) decreases. This decrease is more pronounced as the phase transition surface pressure to the LC phase decreases to zero on the 10 and 20 mol % DMSO subphases. As a result, the LE phase is bypassed on these DMSO subphases and the DPPC monolayers undergo a phase transition from the G phase to the LC phase directly. Mohwald et al. reported similar observations and attributed this effect to the condensing effect of DMSO on DPPC monolayers.[18] The decreased LE to LC phase transition surface pressure is also in agreement with observations[7,14] of an increased main phase transition temperature of the DPPC bilayer, which suggests that DMSO has a stabilization effect on the DPPC condensed phase. Additionally, a similar condensing effect on DPPC films induced by surfactants was previously observed.[40,41]

Although the isotherm of the DPPC monolayer at large MMA is greatly changed by DMSO, the liquid condensed phase is only slightly influenced upon the addition of DMSO. This result suggests that DMSO molecules are squeezed out from the condensed monolayer region. Similar conclusions were also drawn in a previous study on the influence of DMSO on a DPPC bilayer using NMR.[21]

The collapse pressure for each isotherm is also interesting. For a pure water subphase, the DPPC monolayer collapses at about 72 mN/m, which reveals that the DPPC monolayer can reach a near-zero surface tension. This high collapse surface pressure (low surface tension) is consistent with previous isotherm measurements.[42,43] The collapse pressures of the DPPC monolayers on 3, 10, and 20 mol % DMSO subphases are 68, 62, and 56 mN/m, respectively, which are about the same as the surface tensions of each DMSO subphase.[44] This result indicates that near-zero surface tension can also be reached for DPPC monolayers on different DMSO subphases. When the DMSO concentration in a subphase is 40 mol %, the DPPC footprint area in the LC phase shifts much lower (<30 Å^2/molecule, data not shown in Figure 1), indicating a loss of DPPC molecules to the subphase. The bulk solvation of a fraction of the DPPC monolayer in a concentrated 40 mol % DMSO/water subphase is supported by a previous simulation.[27]

Vibrational Sum Frequency Generation Spectroscopy of Dipalmitoylphosphatidylcholine Headgroup. To gain further molecular level insight into the interactions between DPPC and DMSO molecules, VSFG was employed to investigate the phospholipid/aqueous DMSO interface. The headgroup of the DPPC molecule is zwitterionic, consisting of a negatively charged phosphate group and a positively charged choline group. VSFG spectra (*ssp* polarization) of the DPPC phosphate group at different MMAs are shown in Figure 2.

For a pure water subphase, there is no detectable VSFG intensity at low surface coverage (100 Å^2/molecule), as shown in Figure 2. Because VSFG intensity is largely dependent on the orientation and ordering of the molecules, the lack of notable intensity at low surface coverage could be due to a large orientation distribution of the DPPC headgroup in the G−LE region. One peak and a lower energy shoulder are observed when the MMA is compressed to 82 Å^2/molecule (LE phase). The main peak centered at 1094 cm^{-1} is assigned to the headgroup PO_2^- symmetric stretch (SS).[45] The shoulder observed at ~1070 cm^{-1} is not as easy to assign because several possible vibrational modes fall within this frequency region. Since there is no VSFG peak observed for palmitic acid (PA, the chain portion of DPPC; data not shown) in this region, the shoulder is tentatively assigned to a DPPC headgroup C−O stretch. The VSFG spectra are nearly unchanged from the LE to the LE−LC region. Upon further compression to the LC phase (45 Å^2/molecule), the PO_2^- SS peak intensity increases. At the same time, the PO_2^- SS peak shifts from 1094 to 1099 cm^{-1}.

The spectra of the DPPC monolayer on 3 mol % DMSO are similar to the spectra obtained on the water subphase, as shown in Figure 2, indicating no significant influence on the DPPC

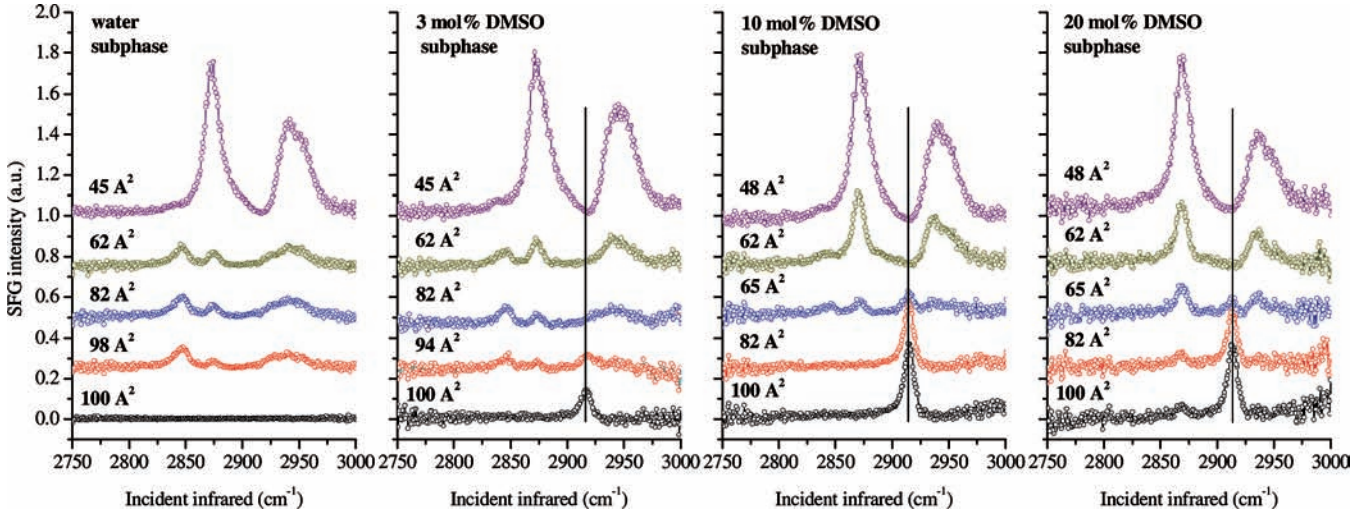

Figure 3. C−H stretch region VSFG spectra of DPPC on different DMSO/water subphases. From left to right, the subphases are water and 3, 10, and 20 mol % DMSO, respectively. The solid line shows the DMSO CH_3 SS peak position. (DPPC is in the LC phase at 45 and 48 Å^2/molecule.)

headgroup by low concentrations of DMSO. However, on 10 and 20 mol % DMSO subphases, the PO_2^- SS peak is observed at 1099 cm^{-1} at all DPPC surface coverages. This blue shift of the vibrational frequency of the phosphate group on concentrated DMSO subphases is direct evidence of a DMSO-induced dehydration of the DPPC headgroup.[31,39]

Water molecules around the DPPC headgroup can be roughly divided into two different categories, bound and free.[46] Bound water molecules participate in the solvation of the headgroup and form the hydration shells around the hydrophilic moieties (such as $-PO_2^-$, $-N(CH_3)_3^+$, and $-C{=}O$) on the headgroup. Free water molecules do not interact in headgroup solvation, although they are still hydrogen bonded to each other. The average number of bound and free water molecules around a single DPPC headgroup in a gel phase bilayer was reported to be 10.8 and 4, respectively.[46] The average number of free water molecules for each headgroup was reported to decrease to 1.1 at 14 mol % DMSO concentration, resulting in a decrease in the intermembrane solvent layer thickness.[17] Additionally, DSC measurements suggested that DMSO molecules do not penetrate into the bound water region when the concentration is below 30 mol %.[47] This result is consistent with our observation in the LC phase (45 and 48 Å^2/molecule) on all subphases in which the PO_2^- SS is observed at 1099 cm^{-1}.

As the MMA increases, the number of water molecules in the solvation shell increases, causing the red shift of the PO_2^- SS frequency to 1094 cm^{-1} because of an increase in hydrogen bonding of water molecules to the phosphate group.[31,48,49] The addition of DMSO to the subphase results in the replacement of water molecules by DMSO molecules at the interface, which leads to the dehydration of the DPPC headgroup at large MMA (82 and 100 Å^2/molecule) for the 10 and 20 mol % DMSO subphases. This is evidenced by the higher frequency of the PO_2^- SS (1099 cm^{-1}). Clearly, DMSO molecules cannot provide the same solvation effect as water molecules to the hydrophilic DPPC headgroup because DMSO does not favor interaction with DPPC headgroups since it is a hydrogen bond acceptor instead of a hydrogen bond donor.

On the 20 mol % DMSO subphase, it is very interesting that the VSFG intensity is notable at large MMA (100 Å^2/molecule), whereas no detectable intensity is observed for water and 3 and 10 mol % DMSO subphases, as shown in Figure 2. This suggests that high concentration of DMSO (>20 mol %) facilitates the aggregation of DPPC molecules and the formation of DPPC domains at the interface because DPPC ordering is observed. Recall that VSFG intensity is sensitive to the order and orientation of the molecules probed. Compared with the 3 and 10 mol % DMSO subphases, the surface tension of the 20 mol % DMSO subphase without lipid coverage is lower (56 mN/m), corresponding to a surface pressure of 16 mN/m relative to pure water. However, the LE to LC phase transition surface pressure for the DPPC monolayer on a water subphase is ~6 mN/m, which is well below the actual surface pressure of the 20 mol % DMSO subphase itself. Therefore, it is reasonable to consider the fact that DMSO molecules act to corral the headgroups into domains at the interface. Therefore, the "pressure" from the DMSO molecules causes the aggregation of DPPC molecules, giving rise to a detectable VSFG intensity.

Vibrational Sum Frequency Generation Spectroscopy of Dipalmitoylphosphatidylcholine Tail Alkyl Chains. VSFG spectra (*ssp* polarization) of DPPC monolayers in the C−H stretching region on different subphases are shown in Figure 3. The structural change of the DPPC monolayer is monitored from the expanded region to the condensed region. For nondeuterated DPPC, both the tail acyl chains and the phosphocholine headgroup contribute to the VSFG spectra. However, because of conformation and orientation issues, VSFG intensity from the headgroup is relatively small compared with the tail groups in spectra with the *ssp* polarization combination. In the spectrum of the condensed DPPC monolayer (45 Å^2/molecule) on a pure water subphase, the small shoulder at 2840 cm^{-1} is assigned to the CH_2 SS of the acyl chains. The peak at 2872 cm^{-1} is assigned to the CH_3 SS of the acyl chains. The small shoulder at ~2905 cm^{-1} is assigned to the CH_2 Fermi resonance (FR) of the acyl chains with a contribution from the CH_2 SS of the phosphocholine headgroup. The peak at ~2942 cm^{-1} is assigned to the CH_3 FR of the acyl chains, and the shoulder at ~2956 cm^{-1} has contribution from the CH_3 asymmetric stretch (AS) of the acyl chains and the CH_2 AS of the headgroup.[50]

Similar to the PO_2^- region, no VSFG intensity is detectable with an MMA of 100 Å^2/molecule on a pure water subphase. When the DPPC monolayer is compressed to 98 Å^2/molecule, surface pressure rises slightly to ~0.5 mN/m, and the VSFG intensity is clearly detected with the CH_2 SS peak at 2844 cm^{-1} and the CH_3 SS peak at 2872 cm^{-1}. The peak intensities of the CH_2 SS and the CH_3 SS in the VSFG spectra contain

information about the conformation and orientation of the acyl chains. The information extracted from the VSFG spectra can be understood on the basis of the symmetry of the vibrational modes, which is related to the nature of VSFG theory. When the CH_2 groups on the acyl chains are disordered and in gauche conformations, they are VSFG active. When the chain changes from a gauche conformation to an all trans conformation, local centers of inversion symmetry appear on the acyl chains, making the CH_2 modes VSFG inactive. For the tail-end CH_3 group, the VSFG intensity depends largely on the orientation angle and its distribution.

The ratio of the intensities of CH_3 SS to CH_2 SS can be used as an indication of monolayer ordering.[32,51–54] As seen in the VSFG spectrum in Figure 3 of a DPPC monolayer at 98 Å^2/molecule on water, the intensity of the CH_2 SS peak is larger than the CH_3 SS peak, indicating that the acyl chains have many gauche conformations. Upon compression of the DPPC monolayer to the LE−LC region, the CH_3 SS peak intensity gradually increases, whereas the CH_2 SS peak intensity is nearly unchanged. A sharp increase in the CH_3 SS peak intensity and a decrease in the CH_2 peak intensity is observed when the DPPC monolayer is compressed to the LC phase (45 Å^2/molecule). The observations above reveal a disordered DPPC monolayer in the LE phase and an ordered DPPC monolayer in the LC phase on a water subphase.

On a 3 mol % DMSO subphase at low surface coverage (100 Å^2/molecule), only the CH_3 SS peak from DMSO at 2914 cm^{-1} is observed. Additionally, the 2914 cm^{-1} peak intensity increases with increasing DMSO surface concentration. However, the observed increase is not as large as was shown in previous VSFG studies of aqueous DMSO[55] without the presence of lipids. Interestingly, when the surface pressure rises to 94 Å^2/molecule, the CH_2 SS and the CH_3 SS peaks from DPPC appear, but the CH_3 SS of DMSO disappears. The vanishing of the DMSO CH_3 SS intensity is also seen on 10 and 20 mol % DMSO subphases when DPPC monolayers are compressed from the G to the LC phase. DPPC CH_3 SS peak intensity appears only on the 20 mol % DMSO subphase at 100 Å^2/molecule (in accordance with the observation in the PO_2^- region).

Condensing Effect by Dimethylsulfoxide. To the limit of our detection, VSFG intensity from DPPC monolayers is discernible at a very low surface number density (120 Å^2/molecule) in both the PO_2^- and the CH regions, as shown Figure 4. It is noteworthy to point out that in the CH region spectrum (Figure 4b), the DPPC CH_3 SS (2872 cm^{-1}) coexists with the DMSO CH_3 SS (2910 cm^{-1}), yet the DPPC CH_2 SS peak is not detectable.

Given the above discussion about the ratio of the peak intensities of the DPPC CH_3 SS and the CH_2 SS, a notable CH_3 SS peak intensity together with lack of a CH_2 SS peak indicates that the DPPC monolayer on a 20 mol % DMSO subphase is well-ordered, even at a very large MMA. The surface covered by DPPC is incomplete at this MMA (120 Å^2/molecule); therefore, we conclude that the DPPC molecules form aggregates and coexist with the DMSO molecules at the interface. Consequently, the occupied molecular area at low surface coverage by each DPPC molecule decreases by adopting ordered chain conformations (fewer gauche defects) on the 20 mol % DMSO subphase. Scheme 2 illustrates disordered DPPC chain conformations on a pure water subphase and ordered DPPC chain conformations on the 20 mol % DMSO subphase.

Chain Orientation of Dipalmitoylphosphatidylcholine in the Liquid Condensed Phase. The chain orientation of DPPC in the liquid condensed phase on different aqueous DMSO subphases was also investigated. Previous studies suggested that the inclination angle of the acyl chains may change by DMSO perturbation.[20] Polarized VSFG spectroscopy is used here to determine the average DPPC chain tilt angle in the ordered monolayers. For a DPPC monolayer with acyl chains in an all trans configuration, the angular relationship between the chain axis and the terminal CH_3 orientation is known to be about 41.5°.[29,56] Therefore, to calculate the DPPC chain tilt angle in the monolayer, the orientation angle of the CH_3 group is needed. This can be obtained by VSFG measurement using the ratio of the CH_3 SS to the CH_3 AS peak intensity in *ssp* polarization spectra.[57]

To avoid the spectral interferences between the terminal CH_3 vibrational modes and other CH moieties of the DPPC molecule, chain deuterated DPPC (DPPC-d_{62}) was used here to determine the terminal methyl group orientation. VSFG spectra (*ssp* polarization) of condensed DPPC-d_{62} monolayers on different subphases are shown in Figure 5. The CD_3 SS and CD_3 AS are observed at 2071 and 2218 cm^{-1}, respectively. The peak at 2121 cm^{-1} is assigned to the CD_3 FR.[31] For a water subphase, the average angle of the CD_3 group calculated from the intensity ratio of the CD_3 SS and the CD_3 AS is 16.5°, so the average chain tilt angle of DPPC-d_{62} is about 25°.[31] This result agrees

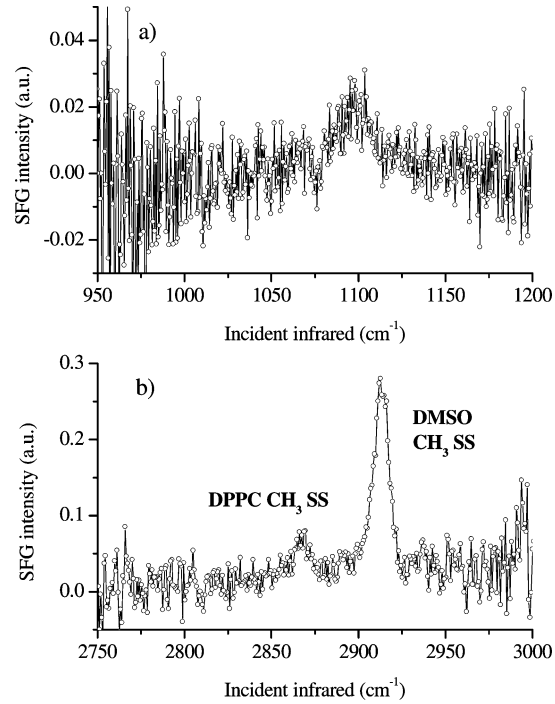

Figure 4. Highlight of the VSFG spectra of DPPC obtained on 20 mol % DMSO subphase at 120 Å^2/molecule in (a) the P═O region and (b) the C−H stretch region.

SCHEME 2: Conformation of DPPC Molecules at Low Surface Coverage (>100 Å^2/molecule) on (a) Water Subphase and (b) 20 mol % DMSO Subphase[a]

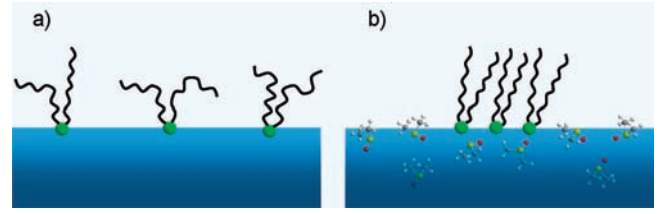

[a] Condensing effect on the DPPC monolayer induced by high-concentration DMSO is illustrated.

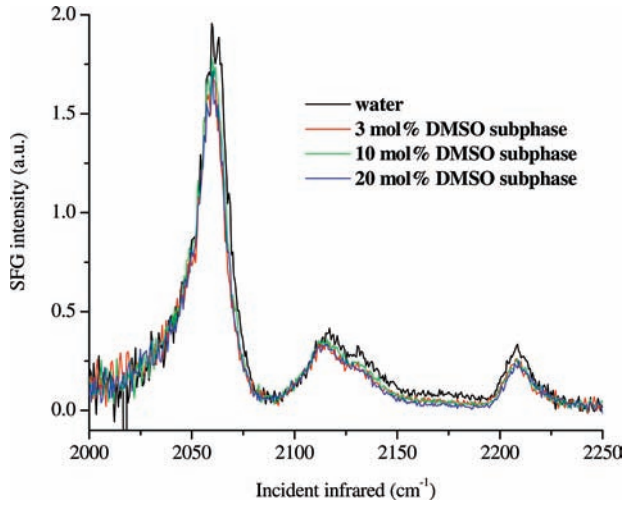

Figure 5. C−D stretch region VSFG spectra of condensed DPPC-d_{62} monolayers on different DMSO/water subphases.

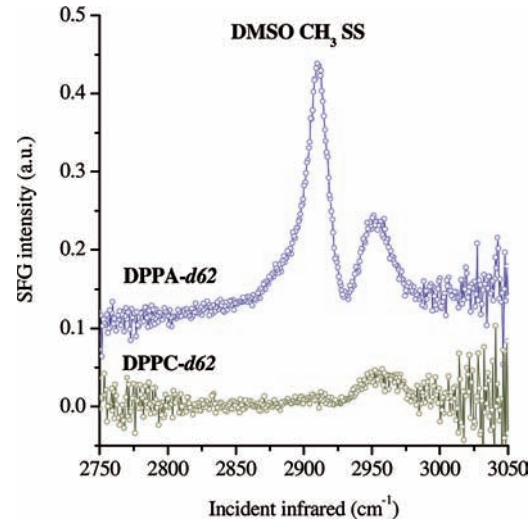

Figure 6. C−H stretch region VSFG spectra of LC phase DPPA-d_{62} and DPPC-d_{62} monolayers on 10 mol % DMSO subphase. The DMSO CH_3 SS peak is absent at the DPPC-d_{62} covered interface.

well with the results obtained by previous X-ray scattering experiments, which gave a value of ∼27°.[58]

The VSFG spectra of the condensed DPPC-d_{62} on DMSO subphases are almost identical to the spectrum obtained on a pure water subphase, indicating an insignificant tilt angle change of the acyl chains upon the addition of DMSO. It should be noted that the VSFG average orientation angle calculation includes the assumption of the angular relationship between the chain and the methyl group, which is different from an X-ray scattering experiment. Our previous VSFG results suggested that the chain orientation of a DPPC monolayer on a water subphase remains nearly unchanged from the LE to the LC phase, but an X-ray scattering study showed an angle decrease from 37 to 29°.[18] With VSFG, the existence of gauche defects in the LE phase complicates the DPPC orientation determination in the LE phase, explaining the discrepancy between the two methods.[31] However, in the work presented here, the orientation determination is of well-packed DPPC molecules in the LC phase, where the acyl chains are in an all trans configuration.

Dimethylsulfoxide Orientation at the Dipalmitoylphosphatidylcholine/Water Interface. The vanishing of the DMSO CH_3 SS peak upon a surface pressure rise (Figure 3) is an interesting phenomenon related to the interaction between the DPPC monolayer and the DMSO molecules. As discussed above, there are arguments about whether the DMSO molecules penetrate into the polar headgroup region or just occupy positions beneath the lipid headgroup. We observe that DMSO molecules exist in the interfacial region. The observed DMSO CH_3 SS peak at low DPPC surface coverage indicates that the DMSO molecules are not completely disordered.

To elucidate the impact of phospholipids on the DMSO molecules, a DPPA-d_{62} monolayer on a 10 mol % DMSO subphase was studied and compared with a DPPC-d_{62} monolayer, as shown in Figure 6. Because the acyl chains of the lipids are deuterated and the DMSO CH_3 SS peak is absent, only CH modes from the lipid headgroup (CH_2 modes: ∼2905 and ∼2956 cm^{-1}) are observed for the DPPC-d_{62} covered interface. However, intensity from the DMSO CH_3 SS peak remains in the VSFG spectrum of the DPPA-d_{62} monolayer. The biggest difference between these two phospholipids is the headgroup charge: DPPC is zwitterionic and DPPA is negatively charged. When the phospholipid monolayer is well packed, the interfacial region is polarized by the electric field induced by the headgroup charge. Previous MD simulation showed that the DPPC molecules adopt an L-shaped conformation in the LC phase, that is, on average a near-flat headgroup orientation with intermolecular charge pairing between the phosphate from one DPPC to the choline of an adjacent DPPC molecule.[59,60] The electric field induced by the DPPC headgroup is therefore nearly parallel to the surface. The DPPA headgroup is negatively charged, and thus the double layer (sodium countercation) creates an electric field along the surface normal of the interface, as illustrated in Scheme 3. Therefore, the DMSO CH_3 SS peak intensity indicates that the polar S═O bond of the DMSO molecules at the monolayer interface is well aligned in the electric field direction. Because the rotation of CH_3 groups about the −S═O bond is allowed, assuming free rotation, the net orientation vector of the CH_3 groups of DMSO is along the −S═O bond axis. Consequently, the DMSO CH_3 orientation vector is nearly parallel and perpendicular to the surface for DPPC and DPPA monolayers, respectively. DMSO orientation in the DPPC system explains the vanishing of the DMSO peak.

SCHEME 3: Illustration of DPPC and DPPA Headgroup Conformation and Charge at the Interface[a]

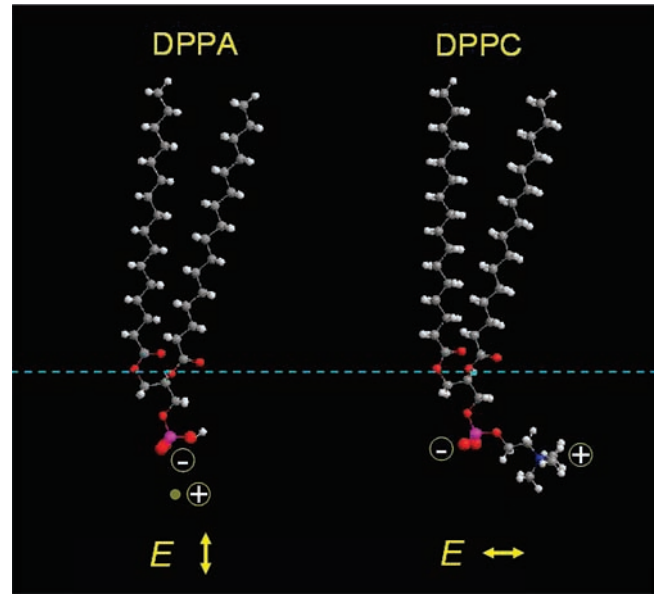

[a] Directions of the headgroup-induced electric fields are also shown.

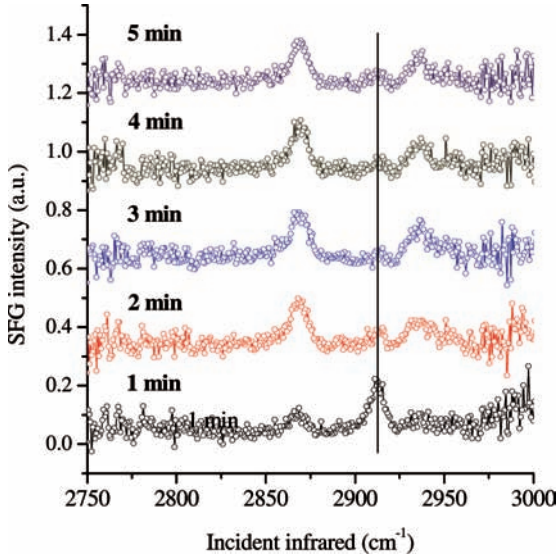

Figure 7. Series of C−H region VSFG spectra of DPPC obtained at the onset of the surface pressure rise on the 20 mol % DMSO subphase. The acquisition time is 1 min for each spectrum. The solid line shows the DMSO CH_3 SS peak position.

(For C_{3v} symmetry, VSFG intensity vanishes at an orientation parallel to the surface in *ssp* and *ppp* polarization.)[61,62] VSFG spectra with *ppp* polarization also reveal the lack DMSO peak intensity (data not shown). The disappearance of DMSO VSFG intensity could also be possible when interfacial DMSO molecules become disordered, although this scenario is unlikely due to the presence of the headgroup-induced electric field.

It should be pointed out that the disappearance of the DMSO peak intensity occurs only after the rise of surface pressure above ~0.5 mN/m. This suggests that a relatively strong electric field is needed to perturb the orientation of the DMSO molecules significantly. Figure 7 reveals the disappearance of the DMSO CH_3 SS peak at 2910 cm^{-1} on the 20 mol % DMSO subphase as a function of time. This result indicates that the surface electric field is established within a few minutes during monolayer compression.

Biological Implications. DMSO interactions play an important role in the enhancement of membrane permeability. Recently, MD simulations of the interaction of DMSO with a model membrane revealed that DMSO molecules induce water pore formation within the lipid bilayer.[26,27] The water pores formed at high DMSO concentration (>10 mol %) were transient and dynamic. From a macroscopic point of view, the existence of the water pores results in an increased area per lipid and a "floppier bilayer". In the present study, the decrease in the area occupied by each DPPC molecule on concentrated DMSO-containing subphases (condensing effect) is observed, which at first appears to be different from the MD simulation results. The pressure that is exerted by DMSO on the DPPC monolayer causes the observed condensing behavior. However, this pressure is also the cause of the pore formation, as shown by MD simulations. DMSO action on the DPPC headgroups is more likely, as compared with action on the DPPC acyl chains because very few DMSO molecules reside in the hydrophobic chain region of lipids.[25] It is then plausible that DMSO acts on the DPPC headgroups to corral the lipids into surface domains. This results in an increase in the average area per lipid in an unconfined system. In a confined system such as a Langmuir trough with rigid barriers, DMSO induces condensing of the lipids. From this argument, our experimental evidence provides support of the pore formation mechanism induced by DMSO and is therefore consistent with the MD simulations. Moreover, previous permeability studies showed that the permeability enhancement induced by DMSO is concentration-dependent and occurs at high concentrations (usually ~60 wt %, or 26 mol %),[10] which is also in accordance with our findings.

Conclusions

A comprehensive picture of the interactions between DMSO molecules and a DPPC monolayer is presented. The impact of DMSO on DPPC monolayers is found to be concentration-dependent. When the DMSO concentration is >10 mol %, DMSO-induced dehydration of the DPPC phosphate group is observed. The high surface pressure of a concentrated DMSO subphase (>20 mol %) induces a condensing effect on the DPPC monolayer, which causes DPPC molecules to adopt a well-ordered conformation at very large MMAs. When DPPC is in the liquid condensed phase, DMSO has an insignificant effect on the monolayer structure, suggesting that DMSO molecules are expelled from the monolayer region. The study of the interaction among DMSO and DPPC and DPPA indicates that the interfacial DMSO molecules are also perturbed by the headgroup-induced electric field and reorient. In summary, our results provide a molecular basis that accounts for the DMSO-induced enhancement of biological membrane permeability.

Acknowledgment. This material is based on work supported by the National Science Foundation under CHE-0749807.

References and Notes

(1) Lovelock, J. E.; Bishop, M. W. H. *Nature* **1959**, *183*, 1394.
(2) Rall, W. F.; Fahy, G. M. *Nature* **1985**, *313*, 573.
(3) Anchordoguy, T. J.; Rudolph, A. S.; Carpenter, J. F.; Crowe, J. H. *Cryobiology* **1987**, *24*, 324.
(4) Anchordoguy, T. J.; Cecchini, C. A.; Crowe, J. H.; Crowe, L. M. *Cryobiology* **1991**, *28*, 467.
(5) Kasai, M. *Reprod. Med. Biol.* **2002**, *1*, 1.
(6) Anchordoguy, T. J.; Carpenter, J. F.; Crowe, J. H.; Crowe, L. M. *Biochim. Biophys. Acta* **1992**, *1104*, 117.
(7) Yu, Z. W.; Quinn, P. J. *Mol. Membr. Biol.* **1998**, *15*, 59.
(8) Neubert, R.; Wohlrab, W.; Marsch, W. *Dermatopharmazie*; Wissenschaftliche Verlagsges: Stuttgart, Germany, 2001.
(9) Barry, B. W. *Nat. Biotechnol.* **2004**, *22*, 165.
(10) Williams, A. C.; Barry, B. W. *Adv. Drug Delivery Rev.* **2004**, *56*, 603.
(11) Ahkong, Q. F.; Fisher, D.; Tampion, W.; Lucy, J. A. *Nature* **1975**, *253*, 194.
(12) Lyman, G. H.; Preisler, H. D.; Papahadjopoulos, D. *Nature* **1976**, *262*, 360.
(13) Yu, Z. W.; Quinn, P. J. *Biosci. Rep.* **1994**, *14*, 259.
(14) Yu, Z. W.; Quinn, P. J. *Biophys. J.* **1995**, *69*, 1456.
(15) Tristram-Nagle, S.; Moore, T.; Petrache, H. I.; Nagle, J. F. *Biochim. Biophys. Acta* **1998**, *1369*, 19.
(16) Long, C. J.; Hmel, P. J.; Kennedy, A.; Quiles, J. G.; Seelbaugh, J.; Reid, T. J. *J. Liposome Res.* **2003**, *13*, 249.
(17) Kiselev, M. A.; Lesieur, P.; Kisselev, A. M.; Grabielle-Madelmond, C.; Ollivon, M. *J. Alloys Compd.* **1999**, *286*, 195.
(18) Krasteva, N.; Vollhardt, D.; Brezesinski, G.; Mohwald, H. *Langmuir* **2001**, *17*, 1209.
(19) Gorshkova, J. E.; Gordeliy, V. I. *Crystallogr. Rep.* **2007**, *52*, 535.
(20) Kiselev, M. A. *Crystallogr. Rep.* **2007**, *52*, 529.
(21) Kennedy, A.; Long, C. J.; Hmel, P. J.; Hicks, R.; Reid, T. J. *Spectrosc.: Int. J.* **2004**, *18*, 265.
(22) Paci, E.; Marchi, M. *Mol. Simul.* **1994**, *14*, 1.
(23) Smondyrev, A. M.; Berkowitz, M. L. *Biophys. J.* **1999**, *76*, 2472.
(24) Sum, A. K.; de Pablo, J. J. *Biophys. J.* **2003**, *85*, 3636.
(25) Leekumjorn, S.; Sum, A. K. *Biochim. Biophys. Acta* **2006**, *1758*, 1751.
(26) Notman, R.; Noro, M.; O'Malley, B.; Anwar, J. *J. Am. Chem. Soc.* **2006**, *128*, 13982.
(27) Gurtovenko, A. A.; Anwar, J. *J. Phys. Chem. B* **2007**, *111*, 10453.
(28) Gordeliy, V. I.; Kiselev, M. A.; Lesieur, P.; Pole, A. V.; Teixeira, J. *Biophys. J.* **1998**, *75*, 2343.
(29) Roke, S.; Schins, J.; Muller, M.; Bonn, M. *Phys. Rev. Lett.* **2003**, 90.

(30) Richmond, G. L.; Walker, R. A.; Smiley, B. L. *Spectroscopy* **1999**, *14*, 18.
(31) Ma, G.; Allen, H. C. *Langmuir* **2006**, *22*, 5341.
(32) Sovago, M.; Wurpel, G. W. H.; Smits, M.; Muller, M.; Bonn, M. *J. Am. Chem. Soc.* **2007**, *129*, 11079.
(33) Liu, J.; Conboy, J. C. *J. Am. Chem. Soc.* **2004**, *126*, 8894.
(34) Anderson, N. A.; Richter, L. J.; Stephenson, J. C.; Briggman, K. A. *Langmuir* **2006**, *22*, 8333.
(35) Anderson, N. A.; Richter, L. J.; Stephenson, J. C.; Briggman, K. A. *J. Am. Chem. Soc.* **2007**, *129*, 2094.
(36) Hommel, E. L.; Ma, G.; Allen, H. C. *Anal. Sci.* **2001**, *17*, 1325.
(37) Ma, G.; Allen, H. C. *J. Phys. Chem. B* **2003**, *107*, 6343.
(38) Tang, C. Y.; Allen, H. C. *J. Phys. Chem. A* **2009**, *113*, 7383.
(39) Ma, G.; Allen, H. C. *Photochem. Photobiol.* **2006**, *82*, 1517.
(40) McConlogue, C. W.; Malamud, D.; Vanderlick, T. K. *Biochim. Biophys. Acta* **1998**, *1372*, 124.
(41) Can, S. Z.; Chang, C. F.; Walker, R. A. *Biochim. Biophys. Acta* **2008**, *1778*, 2368.
(42) Tabak, S. A.; Notter, R. H. *Rev. Sci. Instrum.* **1977**, *48*, 1196.
(43) Notter, R. H.; Tabak, S. A.; Mavis, R. D. *J. Lipid Res.* **1980**, *21*, 10.
(44) Markarian, S. A.; Terzyan, A. M. *J. Chem. Eng. Data* **2007**, *52*, 1704.
(45) Pohle, W.; Selle, C.; Fritzsche, H.; Bohl, M. *J. Mol. Struct.* **1997**, *408*, 273.
(46) Grabiellemadelmont, C.; Perron, R. *J. Colloid Interface Sci.* **1983**, *95*, 483.
(47) Shashkov, S. N.; Kiselev, M. A.; Tioutiounnikov, S. N.; Kiselev, A. M.; Lesieur, P. *Physica B* **1999**, *271*, 184.
(48) Gauger, D. R.; Selle, C.; Fritzsche, H.; Pohle, W. *J. Mol. Struct.* **2001**, *565*, 25.
(49) Mrazkova, E.; Hobza, P.; Bohl, M.; Gauger, D. R.; Pohle, W. *J. Phys. Chem. B* **2005**, *109*, 15126.
(50) Harper, K. L.; Allen, H. C. *Langmuir* **2007**, *23*, 8925.
(51) Walker, R. A.; Conboy, J. C.; Richmond, G. L. *Langmuir* **1997**, *13*, 3070.
(52) Walker, R. A.; Gruetzmacher, J. A.; Richmond, G. L. *J. Am. Chem. Soc.* **1998**, *120*, 6991.
(53) Gurau, M. C.; Lim, S. M.; Castellana, E. T.; Albertorio, F.; Kataoka, S.; Cremer, P. S. *J. Am. Chem. Soc.* **2004**, *126*, 10522.
(54) Liu, J.; Conboy, J. C. *J. Phys. Chem. C* **2007**, *111*, 8988.
(55) Allen, H. C.; Gragson, D. E.; Richmond, G. L. *J. Phys. Chem. B* **1999**, *103*, 660.
(56) Ye, S.; Noda, H.; Nishida, T.; Morita, S.; Osawa, M. *Langmuir* **2004**, *20*, 357.
(57) Ohe, C.; Ida, Y.; Matsumoto, S.; Sasaki, T.; Goto, Y.; Noi, A.; Tsurumaru, T.; Itoh, K. *J. Phys. Chem. B* **2004**, *108*, 18081.
(58) Brezesinski, G.; Dietrich, A.; Struth, B.; Bohm, C.; Bouwman, W. G.; Kjaer, K.; Mohwald, H. *Chem. Phys. Lipids* **1995**, *76*, 145.
(59) Dominguez, H.; Smondyrev, A. M.; Berkowitz, M. L. *J. Phys. Chem. B* **1999**, *103*, 9582.
(60) Cascales, J. J. L.; Otero, T. F.; Smith, B. D.; Gonzalez, C.; Marquez, M. *J. Phys. Chem. B* **2006**, *110*, 2358.
(61) Wang, H. F.; Gan, W.; Lu, R.; Rao, Y.; Wu, B. H. *Int. Rev. Phys. Chem.* **2005**, *24*, 191.
(62) Gan, W.; Wu, D.; Zhang, Z.; Feng, R. R.; Wang, H. F. *J. Chem. Phys.* **2006**, 124.

JP905066W